S0032-3861(96)00167-X

Polymer Vol. 37 No. 16, pp. 3643-3657, 1996
Copyright © 1996 Elsevier Science Ltd
Printed in Great Britain. All rights reserved
0032-3861/96/$15.00+0.00

Reactions of amorphous PE radical-pairs *in vacuo* and in acetylene: a comparison of gel fraction data with Flory–Stockmayer and atomistic modelling analyses

R. A. Jones and I. M. Ward*
IRC in Polymer Science and Technology, Department of Physics, University of Leeds, Leeds LS2 9JT, UK

and D. J. R. Taylor and R. F. T. Stepto
Polymer Science and Technology Group, Manchester Materials Science Centre, University of Manchester and U.M.I.S.T., Grosvenor St., Manchester M1 7HS, UK

(Received 11 October 1995; revised 21 December 1995)

The radiation-induced crosslinking of linear low density polyethylene chains has been analysed theoretically using an atomistic analysis and a Flory–Stockmayer (FS) analysis. Experimentally, gel fractions greater than the theoretical maximum obtainable, assuming every radical reacts to form a crosslink (namely, $D \,.\, G(R)/2$), indicate the occurrence of chain-reactions both in the presence of acetylene and *in vacuo*. Based on previous studies, chain-reaction mechanisms are postulated, involving unterminated polyenes in acetylene and scission-generated vinyls *in vacuo*. Accordingly, numerical comparisons of the theoretical and experimental gel-fraction results, as a function of dose (D), have been used to calculate the number of 'gel-effective' chain-steps per initial alkyl radical generated ($N_{\mathrm{CS,D}}$) for both the atomistic and FS analyses. Both systems of analysis show that, as dose increases, $N_{\mathrm{CS,D}}$ for the acetylene and *in vacuo* results decrease from maximum values at or just after the gel points. The decay is interpreted as resulting from the increased probability of radical–radical termination reactions towards higher levels of dose. Although there are differences between the two analyses, both give essentially the same interpretation of the experimental results. The atomistic analysis predicts maximum values of $N_{\mathrm{CS,D}}$ of 9.0 in the presence of acetylene and 2.9 *in vacuo*. The corresponding values from the FS analysis are 9.4 and 2.8 respectively. As the dose is increased further, the atomistic analysis gives 2.1th- and 2.6th-order decays of $N_{\mathrm{CS,D}}$ as functions of the dose, for the acetylene and *in vacuo* results respectively. The FS analysis gives, correspondingly, 2.6th- and 2.8th-order decays. General equations are developed for irradiated polymers, which relate gel fraction to the dose and the number of initial radicals generated in a pre-irradiated number-average degree of polymerization, via $N_{\mathrm{CS,D}}$. Copyright © 1996 Elsevier Science Ltd.

(Keywords: polyethylene (LLDPE); E-beam irradiation; radical-pairs)

INTRODUCTION

In the experimental analysis of the radiation-induced crosslinking of a linear low density polyethylene (LLDPE) film and high-modulus polyethylene (HMPE) fibres, gel fractions were measured as a function of dose, both *in vacuo* and also in the presence of acetylene gas[1]. It was found that the presence of acetylene appeared to accelerate the crosslinking process, resulting in a reduction in the dose to incipient gelation (D_g), from ca. 1.40×10^4 to 0.42×10^4 Gy or J kg^{-1}, and an increase in the initial rate of gel formation as a function of the dose. Crosslinking was so accelerated by the use of acetylene that the data did not fit Charlesby–Pinner (CP)[2,3] or Saito–Kang–Dole (SKD)[4,5] theories. Closer investigation showed that data from irradiations *in vacuo* also failed to fit CP and SKD theories. SKD theory was developed in order to explain departures from linearity in CP plots derived from PE gel-fraction data. It is based on the premise that such departures result from deviations of the molecular weight distribution functions from 'the most probable distribution', as Wesslau distribution functions. Firstly, λ values ($\lambda = G(S)/2 \,.\, G(X)$; where $G(S)$ and $G(X)$ are the initial radiation efficiency values for scission and crosslinking respectively), determined from the intercepts of CP plots ($=\lambda/2$), were found to increase from the *in vacuo* level with increasing acetylene concentration. Theoretical considerations predict that λ should decrease with increasing acetylene concentration, because $G(S)$ and $G(X)$ are expected to decrease and increase, respectively. In the same paper[1] it was found that chain scissions were largely prevented in the presence of acetylene (1 atm). Secondly, $G(X)$ values determined by SKD theory, from gel fraction curves

---

* To whom correspondence should be addressed

obtained following irradiation *in vacuo* and in the presence of acetylene, were greatly in excess of those expected from the initial numbers of radical-pairs formed (G(R)/2). Thirdly, the SKD-evaluation predicted the rates of crosslink formation to increase with dose in these systems, over almost the entire dose range. This latter point appeared to be inexplicable. More recently, one of us was able to fit the LLDPE and HDPE data, both *in vacuo* and acetylene, to a modification of the Wanxi equation[6]. In order to explain the departures from linearity often encountered when applying CP theory, the Wanxi equation[7] invokes crosslinking and scission densities, which are proportional and inversely proportional, respectively, to a power function of the radiation dose. The Wanxi power function is also dependent upon the polymer structure. In CP theory the crosslinking and scission densities are directly proportional to dose.

Although providing excellent curve-fits for all our data, the Wanxi equation leaves us with a major problem. The radiation efficiency value for the production of alkyl radicals $G(R)$ in polyethylene, was established by Ichikawa *et al.*[8], utilizing the electron spin resonance (e.s.r.) electron-spin-echo (e.s.e.) technique, to be ca. 2.40×10^{-7} mol (spins) J^{-1}. This value was obtained for a medium density PE ($\rho \approx 0.963\,\mathrm{g\,cm^{-3}}$) and it is not expected to change greatly from one type of PE to another. The number of initial radicals (N_R) produced in the linear low dose response region can therefore be found from the expression

$$N_R = G(R) . D . N_C . M_{CH_2} \qquad (1)$$

where D is the dose (Gy), N_C is the total number of methylene units and M_{CH_2} is the formula mass of methylene ($14.026 \times 10^{-3}\,\mathrm{kg\,mol^{-1}}$). Hence, neglecting all radical losses and assuming that every radical pair resulted in one crosslink, it would not be possible to exceed gel fractions, which required greater than N_R radicals (or $D . G(R)/2$ mol(crosslinks) $\mathrm{kg^{-1}}$). All of our experimental gel fraction curves, both *in vacuo* and acetylene (*Figures 1* and *5*), have gel fractions that require greater than $D . G(R)/2$ crosslinks. The only reasonable explanation for this phenomenon is that chain-reactions occur when PE is irradiated and annealed, both *in vacuo* and in acetylene. As will be demonstrated later in this paper, when the Wanxi equation is applied to systems in which chain-reactions occur, fitting yields pseudo G factors which bear no relation to reality. In fact none of the sol–gel equations developed to date allow for chain-reactions and that is really the main reason that they fail completely to describe radiation-induced crosslinking and scission processes.

The non-chain reactions of PE alkyl radicals are described in *Schemes 1* and *2* for annealing *in vacuo* and in acetylene, respectively. The chain-reactions which take place during the *in vacuo* irradiation and annealing of PE can be rationalized as follows. In PE and other solid *n*-hydrocarbon compounds radicals tend to be formed in pairs concomitantly with the liberation of molecular hydrogen[9]. In addition some smaller alkyl species, such as ethane and butane are released. These liberated gases, of which molecular hydrogen is by far the most prevalent[10], facilitate the transfer of radical free sites from one chain to another as 'simple chain-reactions' (*Schemes 3a* and *3b*). A 'chain-reaction' in this case is the number of polymer chains through which the hydrogen atom abstraction reactions pass before termination occurs. The term 'simple chain-reaction' refers to the fact that a radical site has been transferred with no crosslinking or scission reactions taking place. During chain-scission processes *in vacuo*, 'Y-type' crosslinks and terminal vinyls are produced (*Scheme 1*, reaction 1). When a transmitted radical site interacts with one of these terminal vinyl groups a further 'Y-type' crosslink is formed, with transfer of the active radical site to the chain which initially contained the vinyl group (*Scheme 3c*). This is an 'effective chain-step' *in vacuo*. An 'effective chain step' is one in which an inter-chain crosslink occurs as the active radical site is moved from chain to chain. The 'chain-reactions' will continue until radical–radical terminations occur (*Scheme 3d*).

The chain-reactions which take place during the acetylene enhanced crosslinking of PE can be reasoned

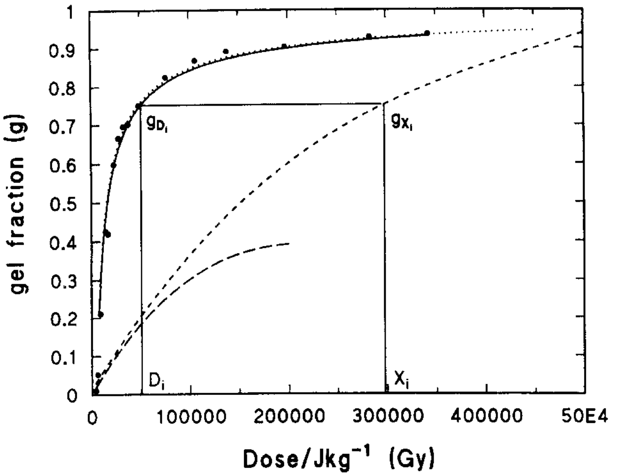

Figure 1 Gel fractions of LLDPE irradiated (18°C) and annealed (100°C) in the presence of acetylene (1 atm), showing: the raw experimental data with modified 'Wanxi' fit (●——); the computed contribution from terminating polyenes (– – –); the computed maximum for all radical-pair terminations as non-chain mediated cross-links, $D . G(R)/2$, (- - - -); and the computed chain-reaction with modified 'Wanxi' fit (· · · · ·)

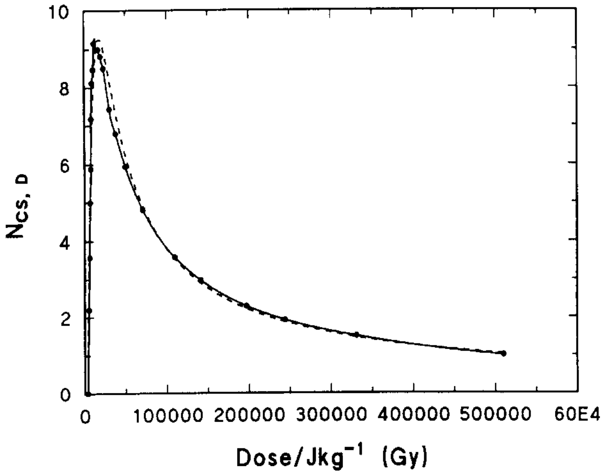

Figure 2 Number of 'gel-effective' chain-steps per termination ($N_{CS,D}$) *versus* dose plot, for the acetylene enhanced irradiation of LLDPE, extrapolated from interpolated experimental gel data and the computed $D . G(R)/2$ gel curve (●——); and $N_{CS,D}$ fitted to equation (5) (- - - -)

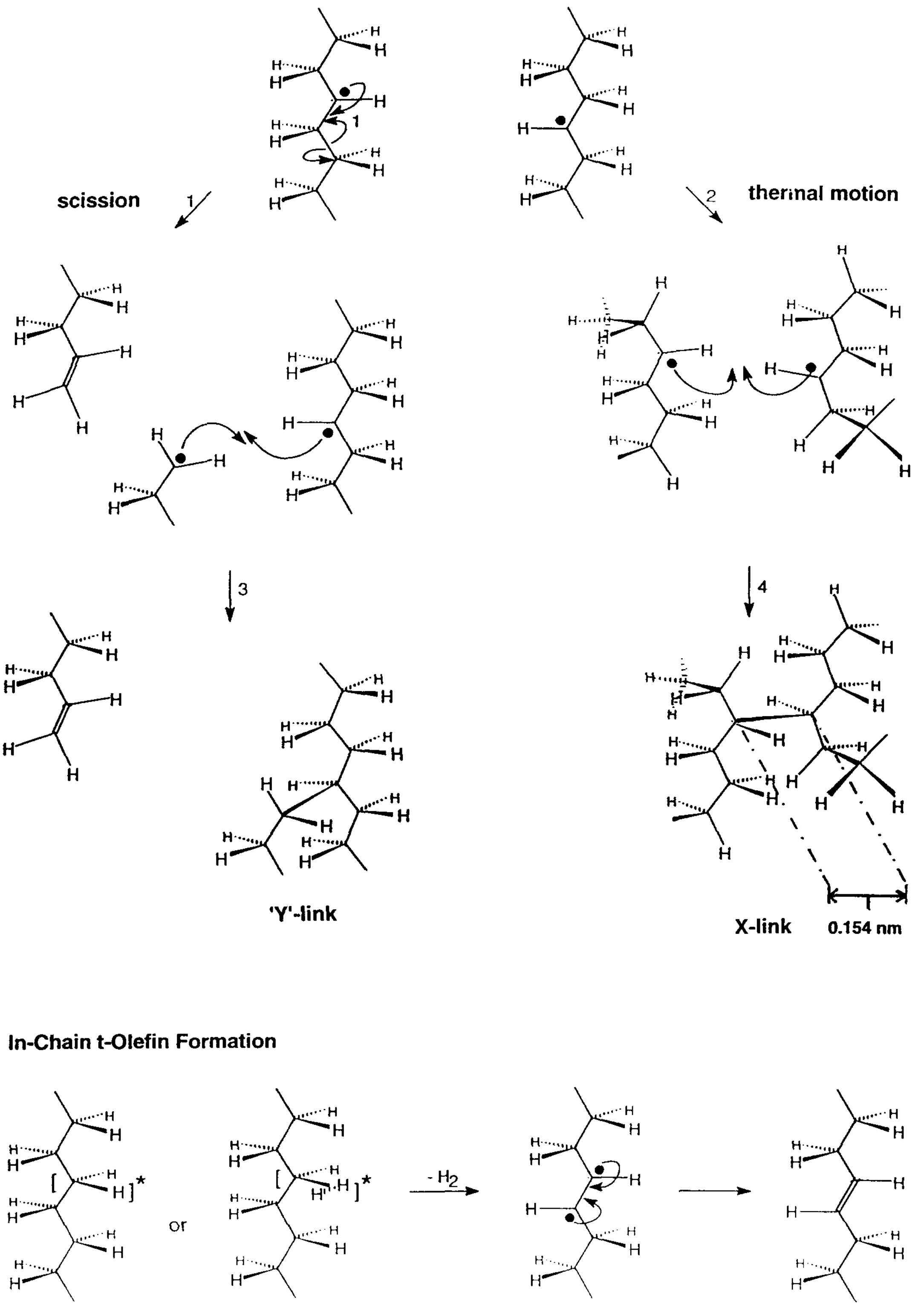

Scheme 1 Reactions of PE alkyl radical pairs *in vacuo*

as follows. In the presence of acetylene, chain scission is almost halted[1] and at 1 atm acetylene the quantities of excised small alkyl groups and molecular hydrogen are negligible. It has been shown that acetylene undergoes addition reactions with alkyl radicals in amorphous PE[1,11] to yield polyene crosslinks (*Scheme 2*). The crosslinks are closed by simple radical–radical termination reactions (*Scheme 2*, reactions 3 and 5). A competing hydrogen atom abstraction reaction has also been observed using Fourier transform infra-red (*FT*i.r.)[12] (*Scheme 2*, reaction 6). By implication, the radical olefin addition reaction (*Scheme 2*, reaction 8) must also exist. Unfortunately, the mechanism is not so simple as had been assumed in the earlier papers[1,11,12]. Often the outgrowing diene or triene adduct radicals do not meet the pair-radical or another radical and terminate, but instead undergo the competing hydrogen atom abstraction reaction (*Schemes 2* and *4*). The reactions may continue

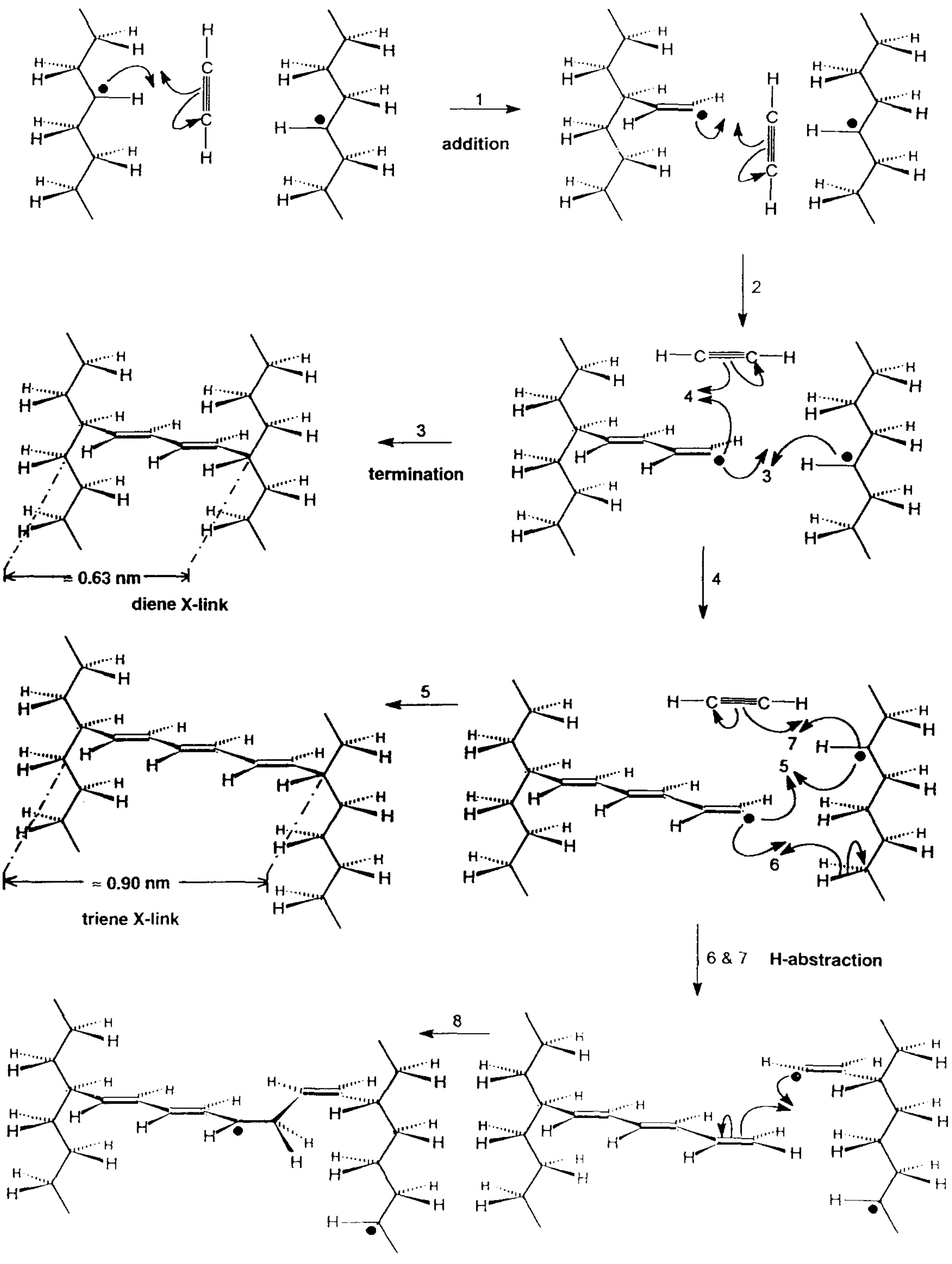

Scheme 2 Reactions of PE alkyl radical pairs with acetylene

as unbranched 'simple chain-reactions', creating non-bridging vinylic polyenes, which are only connected to one chain. Again, the term 'simple chain-reaction' refers to the fact that a radical site has been transferred, via hydrogen atom abstraction, with no crosslinking or scission reactions taking place. Occasionally, unterminated radicals will react with the electron-rich, vinylic, polyenes to yield crosslinks, in which some or all of the polyene character is lost. This is an 'effective chain-step' in acetylene and the radical is not lost, but simply transferred. As *Scheme 4* shows, these 'chain-reactions' will also continue until radical–radical terminations occur.

In a recent publication, we modelled hydrogen-atom ejection and radical-pair formation in amorphous HDPE[9]. Our simple computer model supported experimentally determined mean radical-pair distances in *n*-hydrocarbons and polyethylenes resulting from irradiation[13,14]. The theory of polyene crosslinking termination reactions in amorphous polyethylenes, irradiated in the presence of acetylene (*Scheme 4*)[1,11,12], is also supported, because the mechanism requires the prior formation of radical-pairs

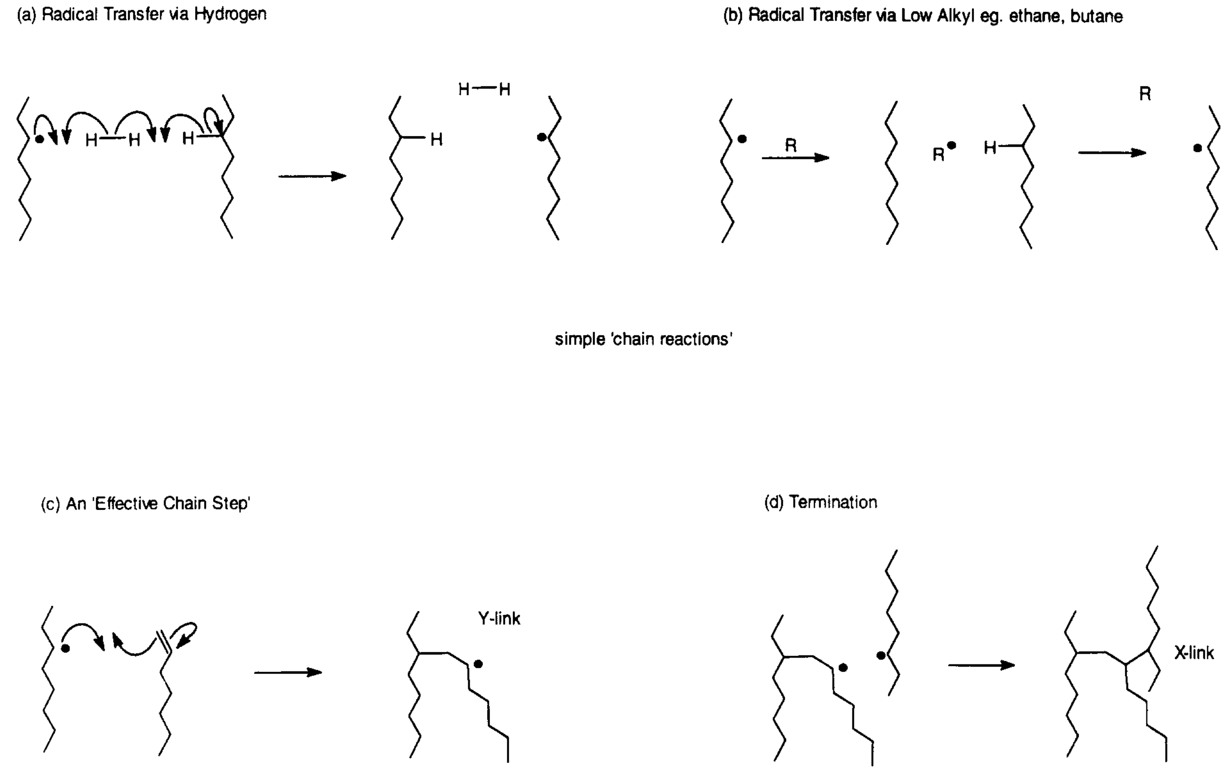

Scheme 3 Chain reactions in amorphous PE irradiated *in vacuo*

which are separated by distances of the order of those found by Dubinskii *et al.*[13]. The simple computer model is applicable to all amorphous solid alkane systems, irrespective of chain branching and density variations, because the techniques employed take account of structural differences. The model has been used as a radical-pair generator in this study of the reactions of radical-pairs in LLDPE. In this paper, the atomistic modelling has been extended to investigate the effects of radiation-induced chain-reactions on crosslinking and gel formation in amorphous LLDPE. Complementary modelling using classical Flory–Stockmayer (FS)

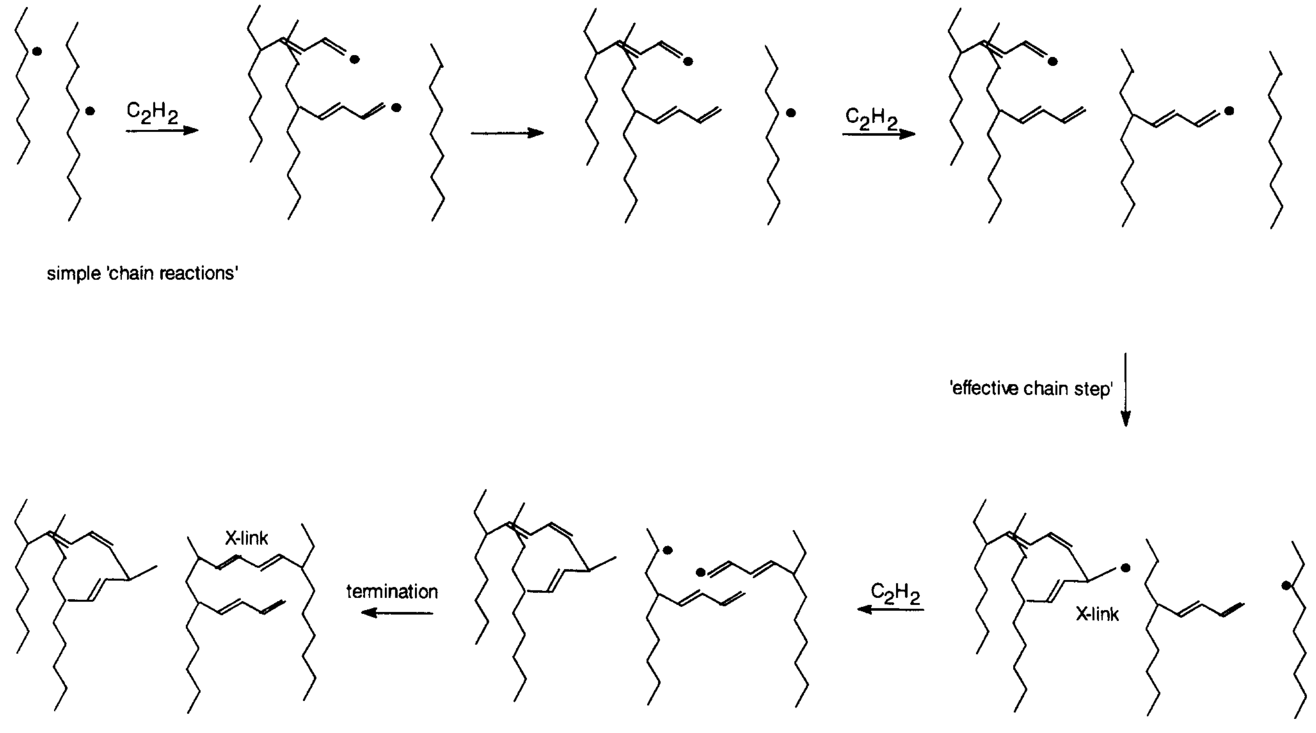

Scheme 4 Chain reactions in amorphous PE irradiated in the presence of acetylene

theory[15,16], modified to account for chain-reactions, is also used to interpret the gel fraction data. This was necessary because none of the sol–gel equations developed to date appear to consider the existence of chain-reactions. The FS treatment of the data is based on the RA_f self-polymerization *via* activated sites in linear polymethylene chains[16]. Gel fraction vs dose data, from the irradiation and annealing of LLDPE *in vacuo* and in the presence of acetylene[1] are analysed. In addition, ultraviolet (u.v.) spectroscopic data[1] concerning the number of terminating polyene crosslinks, formed during the irradiation and annealing of LLDPE in acetylene, have been used. The results are very interesting, allowing us to generate equations to explain gel fractions of irradiated and annealed polymeric alkanes.

EXPERIMENTAL

LLDPE film (thickness 0.126 mm, $\rho = 0.919\,\mathrm{g\,cm^{-3}}$ (gradient column), $M_n = 2.205 \times 10^4$, $M_w = 1.059 \times 10^5$ and $M_z = 2.895 \times 10^5$ (RAPRA Technology Ltd)) was used for the experimental collection of gel-fraction data in this study. All materials and experimental conditions have been described previously in great detail[1]. However, it should be emphasized that, following irradiation (at 18°C) all samples were annealed (at 100°C) in their respective irradiation tube environments (*in vacuo* or in acetylene), before coming into contact with air, so that oxidative degradation was minimized.

ATOMISTIC MODELLING ANALYSIS

Theoretical basis for atomistic modelling

Reactions of radical-pairs were modelled in an amorphous polyethylene macro-cell (BIOSYM Insight II Version 2.3.5, Amorphous Cell 6.1)[17]. A program was written in 'C' to read the Cartesian co-ordinates of the individual atoms in the BIOSYM macro-cell and store the data, relative to the centre of the cell, in one-dimensional arrays. The radical-pair sites were positioned using the method described previously for HDPE[9], with the following exceptions. The initiating radical sites were not placed at the centre of the macro-cell by transposing all remaining atoms relatively around them, and the partner for each initiated radical was selected randomly from the total number of available pairs assigned to that radical. In the absence of literature experimental details, it was also assumed that the parameters which were used to create the LLDPE macro-cell described below, were adequate to describe the LLDPE radical-pair distribution function.

Although LLDPE is not completely amorphous, it is believed that the crosslinks in the crystalline regions are entirely confined to the fold-surface interfaces[18], and that they exist at the surfaces as a direct result of radical migration[19]. Hence, radicals that were initially generated in the crystalline regions migrate to the crystallite interface before reacting. That being the case, it should be possible to use an amorphous macro-cell as an approximation when studying reactions of radical-pairs in semi-crystalline *n*-alkanes. The LLDPE, from which the experimental results were obtained, had a number-average molecular weight corresponding to 1572 methylene (CH_2) groups. Unfortunately, the closest reasonable chain length to this when combined in a suitable BIOSYM macro-cell, 1000 methylene units, yielded only 27 molecules. This number of molecules was insufficient for a statistical treatment of molecular combinations. In addition, with only one chain per unit sub-cell and a high chain-length to sub-cell-length ratio, an unnaturally high degree of chain self-wrapping existed within the cells. Whereas self-wrapping was not a problem when modelling radical-pair formation[9], it is not acceptable for modelling the reactions of radical pairs, because it could influence the intra-chain to inter-chain crosslink ratio. In order to increase the number of molecules available for statistical analysis, it became necessary to reduce the number of methylene units per chain. This necessitated the introduction of a scaling factor, which increased the number of units per chain to that of the LLDPE, by multiplying each methylene unit in the model by the scaling factor. Increasing the chain length in this way prevented the modelling of radical losses, such as those which result from adjacent in-chain radical–radical terminations and *t*-olefin formation (*Scheme 1*). Fortunately, the number of primary radical-pairs lost at any given dose in LLDPE irradiated in the presence of acetylene is known from u.v.-spectroscopy data[1], and the problem may be initially overcome by introducing experimentally determined radical-pair loss factors. To check that the scaling procedure was in fact valid, three different macro-cells were constructed, which contained chain lengths of 50, 100 and 1000 methylene units coupled with scaling factors of 31.44, 15.72 and 1.572 respectively. The scaled chains were thus always equivalent to 1572 methylene units per chain. The macro-cells were given a theoretical dose of 20×10^4 Gy irradiation and the resulting gel fractions agreed to within at worst 2.5%. The computational method of gel determination used is outlined in the next section. The agreement between the cells over the final gel fraction confirms the validity of the scaling approach. The largest difference came from the 1000-methylene-unit chain system and resulted from a statistically insufficient number of molecules, as already described. Use of this chain length at lower doses would be impossible since the error margin would increase. The chains finally selected for modelling the reactions of radical-pairs in LLDPE consisted of 100 carbon atoms. Thirty chains were packed amorphously into each sub-cell at a density of ca. $0.92\,\mathrm{g\,cm^{-3}}$ and equilibrated for 1000 molecular dynamic steps at 293 K. The macro-cells were constructed from eight interlocking sub-cells and, hence, contained 24 000 carbon atoms or 72 480 atoms in total, inclusive of the methylene and methyl (end-group) hydrogens. After scaling the results by a factor of 15.72, the effective number of atoms in the simulation was 1.139386×10^6.

Reactions of radical-pairs with acetylene

In the reaction programs the total number of radicals, for a given dose, generated in the LLDPE macro-cell (N_R) was determined on the basis of equation (1). Since many of the initiating radical-pairs finally terminate as polyene crosslinks in the presence of acetylene[1], our first priority was to convert the u.v.-spectroscopy-measured polyene dose curve (*Figure 3*) into a curve of gel fraction vs dose. The radical-pairs which do not

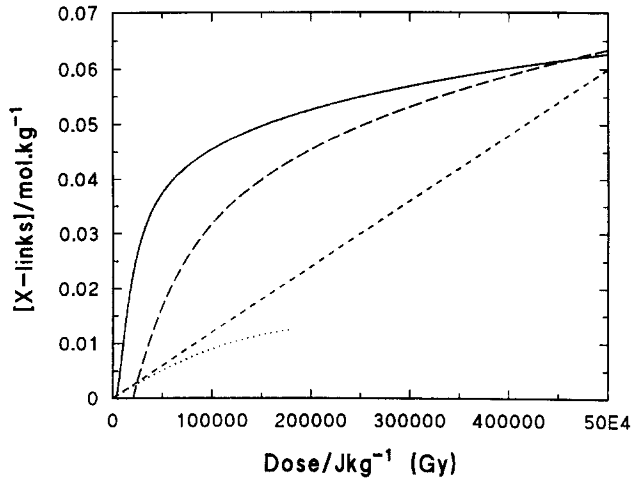

Figure 3 'Gel-effective' crosslink concentration versus dose plots, for irradiated LLDPE, showing; the contribution from terminating polyenes (· · · · ·) resulting from irradiation and annealing in acetylene; the theoretical maximum for all radical-pair terminations as non-chain mediated crosslinks, $D.G(R)/2$, (- - - -); the computed total resulting from chain reactions in acetylene (——); and the computed total resulting from chain reactions *in vacuo* (– – –)

terminate in this way can be considered as losses with respect to polyene formation. 'Radical-losses' arise from reactions such as adjacent radical in-chain terminations (*Scheme 1*). The number of radicals lost at any given dose can be found from *Figure 3*, being the difference between the theoretical $D.G(R)/2$ straight line and the experimental polyene crosslink concentration curve (*Figure 3*). Since N_R is directly proportional to dose, these 'radical-losses' can be fitted to a second-degree polynomial, as far as the data allow (20×10^4 Gy), and the number of radicals which terminate as polyenes in the model LLDPE macro-cell (N_{PR}), can be expressed as

$$N_{PR} = N_R . \{1 - B - (A.D.G(R))\} \qquad (2)$$

where A and B are second-order and first-order radical-loss coefficients. Since, at low doses, the number of polyene crosslinks was approximately equal to the number of radical-pairs, a simple reaction premise was initially devised. It was assumed that: (1) annealing the LLDPE allowed sufficient mobility for radical pairs to meet; (2) diffusion of acetylene gas was relatively uninhibited during annealing, because the same crank-wise segmented chain motions were required for rapid diffusion as were necessary for radical pairs to meet[20]; (3) radical losses could be determined from equation (2); (4) the crosslink to scission probability factor ($p(X)$) was approximately 1 (i.e. negligible scissions); and (5) hydrogen atom abstraction (*Scheme 2*, reaction (6)) was adequately accounted for, because after transfer the radical must eventually crosslink to terminate. Since $p(X) \approx 1$, each radical was crosslinked with its nearest neighbour. Usually, particularly at low doses, this was its pair partner. Crosslinked macromolecules were then accumulated according to size. At the dose to incipient gelation ($D_g \approx 0.388 \times 10^4$ Gy, found by fitting the experimental data to the modified Wanxi equation (8)), only two crosslinks were found on separate pairs of chains in the macrocell. Hence, one crosslink, or two accumulated initial number average chains ($P_{n,0}$), was considered to be the minimum criterion for gel formation. This is the key assumption of the atomistic modelling approach. Errors incurred in making this assumption should really be noticeable only around the gel point. Since the gel-fraction vs dose curves obtained from LLDPE are extremely steep in this region, those errors will be very small. This is a very low degree of crosslinking for gelation, and the results of using this criterion are compared with those found by using the Flory–Stockmayer criterion for gelation later in this paper. The resulting computed polyene gel-fraction curve falls well short of the experimental gel-fraction curve (*Figure 1*), because of the existence of the chain-reactions described earlier. In fact at 20×10^4 Gy, the computed polyene gel fraction is ca. 2.28 × smaller than the experimental value.

Our second objective was to compute the gel fraction curve that would be obtained if all the radicals terminated in crosslink formation with no losses and no intermediate chain-reactions. Apart from not invoking radical-pair losses (equation (2)), this second construct was computationally identical to the first. The resulting computed $D.G(R)/2$ gel-fraction curve also lies well below the experimental gel-fraction curve, over the entire dose range, to 50×10^4 Gy (*Figure 1*), because of the existence of the chain-reactions described previously.

The third objective was to probe the extent of the chain-reaction over the experimental dose range covered. The unique situation of acetylene-enhanced irradiation in amorphous PE with $p(X)$ approximately to 1, affords a method for finding the number of chain-steps which reproduces the experimental gel fraction, or 'gel-effective' chain-steps, per initiating radical ($N_{CS,D}$). For any given dose (D_i) the experimental gel fraction (g_{Di}) is known (*Figure 1*). Extrapolation to the same gel fraction on the $D.G(R)/2$ curve (g_{Xi}), yields the dose (X_i), which would be required to yield g_{Di} if there were no chain-reactions, including all radical losses. The number of radicals produced by the doses D_i and X_i can be obtained from equation (1), and division of the latter by the former yields the average number of 'gel-effective' chain-steps per initiating radical ($N_{CS,D}$). It must be stressed that because $N_{CS,D}$ is developed from experimental gel fraction data, it contains only 'gel-effective' chain-steps. A graph of $N_{CS,D}$ vs dose is given in *Figure 2*. This graph indicates that $N_{CS,D}$ increases dramatically from the gel-point to a maximum of ca. 9.0 at ca. 1.50×10^4 Gy. Unfortunately, the $D.G(R)/2$ curve in *Figure 1* assumes that gel is formed immediately from $D = 0$ onwards, giving rise to a slightly erroneous $N_{CS,D}$ of less than 1 around the gel point. Since $N_{CS,D}$ is also the number of 'gel-effective' crosslinks per initiating radical, it is possible to obtain the maximum chain-reaction, 'gel-effective' radiation pseudo-efficiency value ($G(X_{ChMax}) \approx 10.8 \times 10^{-7}$ mol J^{-1}) by multiplying the maximum $N_{CS,D}$ by $G(R)/2$ (1.2×10^{-7}). This $G(X_{ChMax})$ value is close to the radiation efficiency value for crosslinking calculated in our previous paper ($G(X) = 9.87 \times 10^{-7}$ mol J^{-1})[1], using SKD theory[4,5]. These high pseudo-$G(X)$ values accord with the presence of chain reactions, because they exceed $G(R)/2$. However, the SKD theoretical treatment of our experimental gel fraction results yielded a 'crosslink vs dose' plot in which the $G(X)$ gradient continued to increase with dose beyond the initial value over the entire dose range. As the discussion below shows, this is not possible. From 1.5×10^4 Gy onwards, $N_{CS,D}$ decreases as a 2.1th order reaction with respect to dose. This is very close to second order decay. It is a dose-dependent, rather than time-dependent, decay, because the majority of radicals are frozen until their respective annealing temperatures are reached. Dose becomes the governing factor when annealing is carried out post-irradiation. The maximum appears because of two competing processes. Firstly, $N_{CS,D}$ rapidly increases with the increase in non-crosslinking, vinylic-unsaturation produced by radical addition to acetylene. Secondly, as the radical concentration is raised, by increasing the dose further, decay of $N_{CS,D}$ sets in. Since only 'gel-effective' chain steps are considered, the decay in $N_{CS,D}$ is purely related to the increased propensity for radical–radical termination and not crosslink redundancy. A crosslink is redundant if it connects to a chain which is already part of a network. Termination of two radicals results in the loss of further intermediate chain-steps, which would have arisen from them if radical transfer reactions had continued. Usually, $N_{CS,D}$ includes the effect of scissions and crosslinks as

$$N_{CS,D} = N_{XT,D} - N_{ST,D} \qquad (3)$$

where $N_{XT,D}$ is the number of 'gel-effective' crosslinks per termination and $N_{ST,D}$ is the number of 'gel-effective' scissions per termination. In the presence of acetylene, $N_{CS,D}$ was assumed to be equal to $N_{XT,D}$ because the number of chain scissions is negligible ($p(X) \approx 1$). Since the decay of $N_{CS,D}$ is approximately second order, it was fitted over the entire dose range (*Figure 2*), with an equation which was developed from a dose-dependent second order rate equation. A true second order decay with respect to dose would conform to the equation

$$N_{CS,D} = \frac{N_{CS,0}}{(N_{CS,0} \cdot k_2 \cdot D) + 1} \qquad (4)$$

where $N_{CS,0}$ is the initial number of maximum 'gel-effective' chain-steps at an infinitely small dose and k_2 is the second order rate constant. However, because of the initial increase of $N_{CS,D}$ in this case, $N_{CS,0}$ cannot be considered as a constant, and was found to increase as $K_1 \cdot D'^{a}$, where D' is the dose in excess of that required for incipient gelation ($D' = D - D_g$), a and K_1 are constants. It is more convenient to express $k_2 \cdot D$ as $K_2 \cdot D'^{a}$, where K_2 is a constant. Hence, we arrive at the fit equation which takes the form

$$N_{CS,D} = \frac{K_1 \cdot D'^{a}}{\{K_1 \cdot K_2 \cdot D'^{2.a} + 1\}} \qquad (5)$$

and yielded least-squares values of $a \approx 0.811$, $K_1 \approx 7.93 \times 10^{-3}\,\mathrm{Gy}^{-a}$ and $K_2 \approx 2.30 \times 10^{-5}\,\mathrm{Gy}^{-a}$.

The easiest way to incorporate the effect of the chain-reactions into our computer-model according to equation (5), was to invoke a hypothetical pseudo-effective number of radicals ($N_{ER,D}$)

$$N_{ER,D} = N_{CS,D} \cdot N_R \qquad (6)$$

which when reacted individually, without intermediate chain reactions, created the equivalent total number of crosslinks ($N_{X,D}$) found following the chain-reactions and terminations in acetylene at a given dose

$$N_{X,D} = N_{CS,D} \cdot \frac{N_R}{2} \qquad (7)$$

The radical-pair reaction program was modified to do this and a third computer gel-fraction curve produced. This curve, also shown in *Figure 1*, almost exactly fits the experimental data, as it should. Fitting the modified Wanxi equation[6] to the data in *Figure 1*

$$g_D = \frac{(1 - L \cdot D^{(\beta-1)}) + \sqrt{(2 \cdot L \cdot D^{(\beta-1)} + 1)}}{2} \qquad (8)$$

yields values of $\beta = 0.573$ and $L = 151.5$. In this equation g_D is the gel fraction at dose D, β is related to polymer structure and L is supposed to be equivalent to $G(S)/G(X)$. However, L cannot be equivalent to $G(S)/G(X)$, because it should have a value approaching the CP theory prediction of 0.462 for acetylene enhanced irradiation[1]. The constant L is therefore more complex than $G(S)/G(X)$.

The 'gel-effective' concentration of crosslinks at any given dose ($[X_{eff,D}]$), which computationally reproduced the experimental gel-fraction curve was calculated from $N_{CS,D}$. As a consequence of equation (3), $[X_{eff,D}]$ usually results from the total number of 'gel-effective' crosslinks $[X_{T,D}]$ and the total number of 'gel-effective' scissions $[S_{T,D}]$ as

$$[X_{eff,D}] = [X_{T,D}] - [S_{T,D}] \qquad (9)$$

However, since $[S_{T,D}]$ is assumed to be negligible when acetylene is present, $[X_{eff,D}]$ was assumed to be equal to $[X_{T,D}]$. Hence, $[X_{eff,D}]$ can be expressed in terms of the chain-reactions as

$$\begin{aligned}[X_{eff,D}] &= D \cdot \frac{G(R)}{2} \cdot N_{CS,D} \\ &= D \cdot \frac{G(R)}{2} \cdot \frac{K_1 \cdot D'^{a}}{\{K_1 \cdot K_2 \cdot D'^{2a} + 1\}} \qquad (10)\end{aligned}$$

The $[X_{T,D}]$ vs dose curve, which computationally reproduced the experimental gel fraction, is shown in *Figure 3*, together with the terminating polyene crosslink concentration curve ($[P_X]$) and the theoretical maximum $D \cdot G(R)/2$ concentration gradient for the absence of chain-reactions. The impact of the acetylene enhanced 'gel-effective' chain-reactions can now be quantitatively seen. At 18.0×10^4 Gy $[P_X]$ contributes only ca. 24.6% to the total $[X_T]$. In fact the actual number of crosslinks must be even higher and probably not tending to a plateau, because we have only determined those which are 'gel-effective'.

The number of 'gel-effective' crosslinks ($N_{Xeff,D}$) is related to the total number of crosslinks ($N_{X,D}$) and scissions ($N_{S,D}$), which produce the gel fraction at any given dose

$$N_{Xeff,D} = N_{X,D} - N_{S,D} \qquad (11)$$

Since we have the unique situation of virtually no scissions when PE is irradiated in the presence of acetylene ($(N_{Xeff,D}) \approx (N_{X,D})$), it is possible to plot gel fractions as a function of the number of 'gel-effective' crosslinks per initial number average molecule

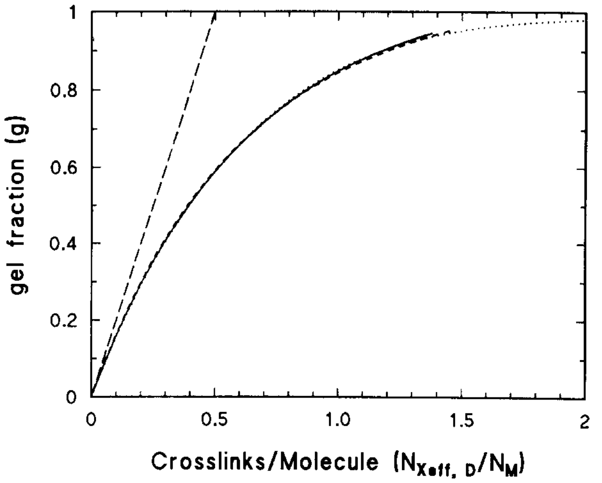

Figure 4 Gel fraction *versus* $N_{\text{Xeff},\text{D}}/N_{\text{M}}$ plots, for irradiated LLDPE, showing; the computed $N_{\text{X},\text{D}}/N_{\text{M}}$ plot resulting from irradiation and annealing in acetylene, using equation (12) (——); the computed $N_{\text{Xeff},\text{D}}/N_{\text{M}}$ plot resulting from irradiation and annealing *in vacuo*, using equation (12) (- - - -); the $g_{\text{D}}/N_{\text{X},\text{SM}}/N_{\text{M}}$ gradient (– – –), which represents the statistical minimum arrangement of connections of pre-irradiation number-average molecules, once only to one other molecule, via 'gel-effective' crosslinks; and the computed $N_{\text{Xeff},\text{D}}/N_{\text{M}}$ plot for the LLDPE extended beyond current data, using equation (12), towards gel fraction unity (- - - -)

($N_{\text{X},\text{D}}/N_{\text{M}}$, where N_{M} is the total number of molecules in the BIOSYM macro-cells). This was done for the data from our computational reproduction of the experimental gel fractions (*Figure 4*, solid curve). Also included in *Figure 4* (dashed line) is the gel fraction vs $2 . N_{\text{X},\text{SM}}/N_{\text{M}}$ plot which represents the statistical minimum arrangement of crosslinks required to achieve a given gel fraction, assuming that the molecules are connected only once via 'gel-effective' crosslinks to one other molecule without networking or redundancy. The gel-fraction *versus* $2 . N_{\text{X},\text{SM}}/N_{\text{M}}$ plot has been included because initially, at low doses, the atomistic model assumes that the gel fraction is made up of single non-networked 'gel-effective' crosslinks, which connect pairs of pre-irradiation number-average molecules. If all the molecules were connected once, without networking or crosslink redundancy, $N_{\text{X},\text{SM}}/N_{\text{M}}$ would equal 0.5 at a gel fraction of 1. Hence, in the statistical minimum arrangement of crosslinks the gel fraction (g_{D}) would be equal to $2 . N_{\text{X},\text{SM}}/N_{\text{M}}$. The computer-simulated g_{D} *versus* $N_{\text{X},\text{D}}/N_{\text{M}}$ curve (*Figure 4*, solid curve), deviates negatively and exponentially from the $g_{\text{D}}/N_{\text{X},\text{SM}}/N_{\text{M}}$ gradient according to the following expression

$$g_{\text{D}} = 2 . \frac{N_{\text{X},\text{D}}}{N_{\text{M}}} . \left\{ K_3 . \exp\left(-b . \frac{N_{\text{X},\text{D}}}{N_{\text{M}}} \right) + C \right\} \qquad (12)$$

yielding; pre-exponential constant $K_3 = 0.697$, exponential constant $b = 0.963$ and constant $C = 0.158$. The deviation of the gel fraction from the initial $g_{\text{D}}/N_{\text{X},\text{SM}}/N_{\text{M}}$ gradient occurs because the number of 'gel-effective' crosslinks required to achieve it exponentially increases from the minimum possible statistical arrangement. The constants in equation (12) are, therefore, probably related to spatial and physical arrangements of the pre-irradiated polymer molecules, such as length, branching, folding and crystallinity of the chains and also the number of chains per unit volume. The dotted curve in *Figure 4* is an extension of the $N_{\text{X},\text{D}}/N_{\text{M}}$ plot, obtained from equation (12), beyond current experimental data towards gel-fraction unity. It is almost impossible to collect data at these higher $N_{\text{X},\text{D}}/N_{\text{M}}$ ratios, because of the doses required to achieve them. From equations (1), (7) and (10) it can be seen that $N_{\text{X},\text{D}}/N_{\text{M}}$ can also be expressed as

$$\frac{N_{\text{X},\text{D}}}{N_{\text{M}}} = [X_{\text{eff},\text{D}}] . \frac{M_{\text{n},0}}{10^3} \qquad (13)$$

where $M_{\text{n},0}$ kg mol^{-1} is the pre-irradiated number-average molecular weight of the polymer. Combination of equations (10), (12) and (13) allows the production of a generalized equation for gel fractions in terms of dose

$$\begin{aligned} g_{\text{D}} = {} & \left(\frac{D . G(R) . M_{\text{n},0}}{10^3} \right) . \left(\frac{K_1 . D'^{\text{a}}}{K_1 . D_2 . D'^{2.\text{a}} + 1} \right) . \\ & \times \left\{ K_3 . \exp\left(-b . \left(\frac{D . G(R) . M_{\text{n},0}}{2 \times 10^3} \right) . \right. \right. \\ & \left. \left. \times \left(\frac{K_1 . D'^{\text{a}}}{K_1 . K_2 . D'^{2.\text{a}} + 1} \right) \right) + C \right\} \end{aligned} \qquad (14)$$

or more simply by substituting for $N_{\text{CS},\text{D}}$ from equation (5)

$$\begin{aligned} g_{\text{D}} = {} & \left(\frac{D . G(R) . M_{\text{n},0} . N_{\text{CS},\text{D}}}{10^3} \right) . \\ & \times \left\{ K_3 . \exp\left(-b . \left(\frac{D . G(R) . M_{\text{n},0} . N_{\text{CS},\text{D}}}{2 \times 10^3} \right) \right) + C \right\} \end{aligned} \qquad (14.1)$$

This equation relates the gel fraction to the dose, the number of initial radicals generated, the pre-irradiation number-average chain molar mass, and the average number of 'gel-effective' chain-steps per termination. It also describes the number of 'gel-effective' crosslinks required to achieve the gel fraction, as an exponential deviation from the minimum possible statistical arrangement.

Reactions of radical-pairs in vacuo

As stated in the Introduction, chain-reactions of a somewhat different nature take place *in vacuo*. They also result in much higher experimental gel fractions than those predicted by the $D . G(R)/2$ curve (*Figure 5*), over almost the entire dose range. The $D . G(R)/2$ curve again represents the theoretical maximum gel fraction obtainable, if all the radical-pairs terminated in crosslinks without intermediate chain-reactions. The presence of chain-reactions *in vacuo* enabled us to repeat the same analytical procedure, used when acetylene was present, to obtain $N_{\text{CS},\text{D}}$. However, since scissions occur to a considerable degree *in vacuo* they cannot be ignored. During chain scission a radical and a terminal vinyl are created (*Scheme 1*, reaction 1), so the radical is transferred and the net $N_{\text{ER},\text{D}}$ can be considered as before. However, in this case $N_{\text{ER},\text{D}}$ and $N_{\text{CS},\text{D}}$ also

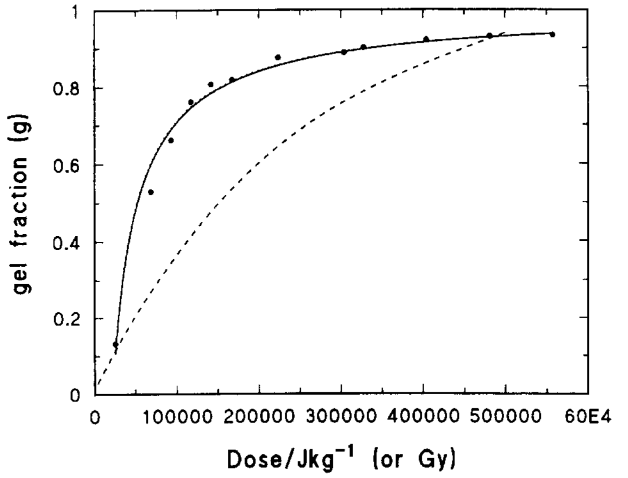

Figure 5 Gel fractions of LLDPE irradiated (18°C) and annealed (100°C) *in vacuo*, showing: the raw experimental data with modified 'Wanxi' fit (● ——); the computed maximum for all radical-pair terminations as non-chain mediated cross-links, $D\,.\,G(R)/2$, (- - - -); and the computed chain-reaction with modified 'Wanxi' fit (· · · · ·)

include the result of 'gel-effective' scissions (equations (3) and (6)). The 'gel-effective' crosslinks and scissions are directly related, because the 'gel-effective' chain-step crosslinks form directly on vinyl scission fragments. The resulting *in vacuo* $N_{\mathrm{CS,D}}$ vs dose curve (*Figure 6*), is of the same form as that produced for acetylene, yielding constants of $a = 0.688$, $K_1 = 3.75 \times 10^{-3}\,\mathrm{Gy}^{-a}$ and $K_2 = 1.13 \times 10^{-4}\,\mathrm{Gy}^{-a}$ from equation (5). It can be seen immediately from this curve that the maximum $N_{\mathrm{CS,D}}$ *in vacuo* is more than three times smaller than when acetylene was present. There are two reasons for this phenomenon. Firstly, $N_{\mathrm{CS,D}}$ includes 'gel-effective' chain scission (equation (3)). Secondly, the *in-vacuo* chain-reaction mechanism is not so effective as the one operating in the presence of acetylene. The latter point may be explained by the lower concentrations of molecular hydrogen and small excised alkyls, compared to the higher concentration of acetylene when it is used. It must also be remembered that a 'gel-effective' chain-step *in vacuo* requires the presence of a terminal vinyl group and a much higher dose is needed to produce the concentration of terminal vinyl groups, compared to the production of unsaturation when acetylene is present. This is reflected in the higher dose-to-incipient-gelation *in vacuo* ($D_g = 2.12 \times 10^4$ Gy). As was previously encountered in acetylene, after reaching a maximum, $N_{\mathrm{CS,D}}$ decreases towards unity at higher doses, because of the increasing ease of termination. For the initial low-dose portion of the *in-vacuo* curve, where radical-pairs are widely spaced, the following approximation can be made. With the exception of the termination reaction, a scission is required before an effective crosslink can be formed. Hence, the number of scissions can be expressed as follows

$$N_{\mathrm{ST,D}} = N_{\mathrm{CS,D}} - 1 \qquad (15)$$

The −1 is present because the termination reaction does not require a vinyl producing chain scission. Since $N_{\mathrm{CS,D}}(\mathrm{max.}) = 2.87$, then from equation (15) $N_{\mathrm{ST,D}}(\mathrm{max.}) = 1.87$ and from equation (3), $N_{\mathrm{XT,D}}(\mathrm{max.}) = 4.75$. It now becomes possible to obtain the maximum chain-reaction, pseudo-efficiency, G values for 'gel-effective' scissions ($G(S_{\mathrm{ChMax}}) = 2.25 \times 10^{-7}\,\mathrm{mol\,J^{-1}}$) and crosslinks ($G(X_{\mathrm{ChMax}}) = 5.69 \times 10^{-7}\,\mathrm{mol\,J^{-1}}$), by multiplying $N_{\mathrm{ST,D}}$ and $N_{\mathrm{XT,D}}$ by $G(R)/2$, as for acetylene previously. It is interesting to note that these pseudo-G values now give $G(S_{\mathrm{ChMax}})/G(X_{\mathrm{ChMax}})$ as ca. 0.4. CP theory, which is still thought to be valid *in vacuo* at the intercept of the CP plot[1], also predicts a value for $G(S)/G(X)$ of ca. 0.4. By substituting for $N_{\mathrm{CS,D}}$ from equation (15) into equation (3), it can be seen that $N_{\mathrm{XT,D}}$ is always greater than twice $N_{\mathrm{ST,D}}$ for the initial near-linear portion of the *in vacuo* $N_{\mathrm{CS,D}}$ vs dose curve, under the conditions described here

$$N_{\mathrm{XT,D}} = 1 + 2\,.\,N_{\mathrm{ST,D}} \qquad (16)$$

The effect of the chain-reactions was incorporated into the model, as before, by invoking a hypothetical pseudo-effective number of radicals based on the constants a, K_1 and K_2 obtained from fitting equation (5) to the *in-vacuo* data. The resulting computer-simulated gel-fraction curve (*Figure 5*) fits the experimental gel-fraction curve well, yielding values of $\beta = 0.426$ and $L = 675.8$ from the modified Wanxi equation (8). As for the acetylene case, the L value is very high and therefore, more complex than merely $G(S)/G(X)$.

Having again established the validity of using a pseudo-effective number of radicals to describe the experimental gel fractions via our computer model, the $[X_{\mathrm{eff,D}}]$ vs dose curve (*Figure 3*) was calculated using equation (10). In this case $[X_{\mathrm{eff,D}}]$ includes the effect of scissions as described by equation (9). Comparison with the $D\,.\,G(R)/2$ line, also shown in *Figure 3*, demonstrates the magnitude of the *in-vacuo* chain reactions.

An *in-vacuo* g_{D} vs $N_{\mathrm{Xeff,D}}/N_{\mathrm{M}}$ plot was then generated (*Figure 4*). Since $N_{\mathrm{Xeff,D}}$ includes the effect of scission (equation (11)), there was no need to correct N_{M} for the total number of scission fragments. A true *in-vacuo* g_{D} vs $N_{\mathrm{X,D}}/N_{\mathrm{M}}$ plot would need to be corrected for the total number of scission fragments. Within experimental error this *in-vacuo* plot matches the plot obtained from the acetylene-gassed system and conforms to the gel equations (equations (12), (14) or (14.1), with $N_{\mathrm{Xeff,D}}$ instead of $N_{\mathrm{X,D}}$ where appropriate), as can be seen from the near identical fitting constants; $K_3 = 0.708$, $b = 1.03$

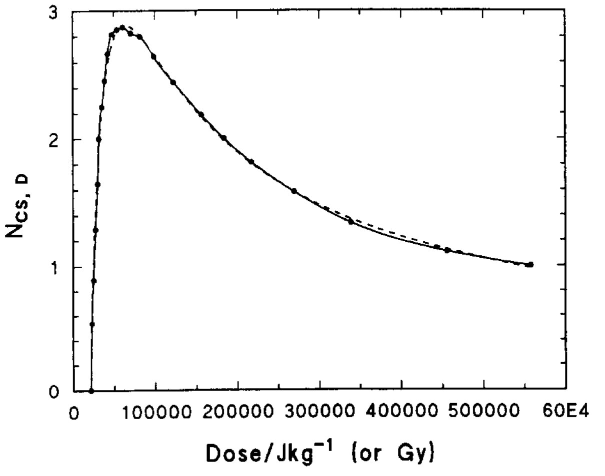

Figure 6 Number of 'gel-effective' chain-steps per termination ($N_{\mathrm{CS,D}}$) vs dose plot, for the *in-vacuo* irradiation of LLDPE, extrapolated from interpolated experimental gel data and the computed $D\,.\,G(R)/2$ gel curve (●——); and $N_{\mathrm{CS,D}}$ fitted to equation (5) (- - - -)

and $C = 0.169$ (cf. in acetylene $K_3 = 0.697$, $b = 0.963$ and constant $C = 0.158$). This is to be expected, because the constants probably relate to the physical arrangements of the pre-irradiated LLDPE polymer chains, and the same atomistic macro-cell was used for the analysis of both sets of irradiation conditions. The method of treatment is therefore also applicable to *in-vacuo* systems following irradiation, within the limitation that $N_{\mathrm{Xeff,D}}$ and $[X_{\mathrm{eff,D}}]$ include 'gel-effective' chain scissions (equations (9) and (11)).

FLORY–STOCKMAYER ANALYSIS

Theoretical basis of Flory–Stockmayer analysis

The gelation analysis used in this section, is based on the Flory–Stockmayer (FS) treatment, of an RA_f (polyfunctional) self-polymerization[15,16]. FS theory provides a basic explanation of gelation phenomena, to which the behaviour and changes in actual crosslinking reactions may be related. The fundamental assumptions implicit in the use of FS theory are: (i) intermolecular crosslinking reactions occur completely at random; (ii) no pre-gel intra-molecular reaction occurs (no crosslinks between reactive sites on the same molecule before the gel point); (iii) post-gel intramolecular reactions (redundancies) in the gel molecules are allowed. For the purposes of the FS theory, the independent variable is the extent of reaction p, where

$$p = \frac{\text{number of sites reacted}}{\text{total number of sites}} \qquad (17)$$

In the case of LLDPE, each methylene unit constitutes a reactive 'site', which can form a $-{}^{\bullet}\mathrm{CH}-$ radical. It is assumed that every radical so-formed, always gives rise to a crosslink. (In relation to the atomistic modelling analysis above; $p = N_{\mathrm{ER}}/N_{\mathrm{C}}$ or $\approx N_{\mathrm{R}}/N_{\mathrm{C}}$ in the presence of acetylene.) The effects of possible chain-scission are ignored, thus allowing p to be related to the equivalent radiation dose

$$D_{\mathrm{FS}} = \frac{p}{G(R)\,.\,M_{\mathrm{CH_2}}} \qquad (18)$$

where D_{FS} is the FS dose corresponding to an extent of reaction p, in the FS model. In order to calculate the gel fraction as a function of radiation dose the following expressions are required (initially in terms of p)[16]. In FS theory, the gel point is defined as the point at which a covalently-linked infinite network first occurs, giving the extent of reaction at gel (p_{g}) as

$$p_{\mathrm{g}} = \frac{1}{(f_{\mathrm{w}} - 1)} \qquad (19)$$

where f_{w} is the weight-average functionality[15], or number of $-\mathrm{CH_2}-$ groups, of the molecule with molar mass equal to the weight-average molar mass (M_{w}) of the sample. In the present case, $M_{\mathrm{w}} = 1.059 \times 10^5$, hence $f_{\mathrm{w}} = 7550$. The gel fraction increases from zero at the gel point, to a limiting value of 1 at complete reaction, at which point all the starting molecules are crosslinked to form a single, infinite 'gel' molecule. However, the infinite molecular species cannot be enumerated, and the gel fraction (g) must be found by calculating the complementary quantity, the unit-fraction of sol (s), from

$$g = 1 - s \qquad (20)$$

s is formed by summing over all the finite (defined) molecular species

$$S = \sum_{x=1}^{\infty} u_{\mathrm{x}} \qquad (21)$$

where u_{x} is the unit-fraction of the species with degree of polymerization x. For an RA_f polymerization and for a particular value of x, u_{x} is given by

$$u_{\mathrm{x}} = \frac{x\,.\,(1-p)^2}{p} \cdot \frac{f\,.\,[x\,.\,(f-1)]!}{[x\,.\,(f-2)+2]!\,.\,x!} \cdot \beta^{\mathrm{x}} \qquad (22)$$

where $f = f_{\mathrm{w}}$ and

$$\beta = p\,.\,(1-p)^{(f-2)} \qquad (23)$$

The combinatorial factor in equation (22) accounts for the number of distinct isomers of molecular species with defined structures of x units, i.e. those with $[x\,.\,(f-2)+2]$ unreacted sites. Performing the summation in equation (21), yields the final expression for s, for an RA_f polymerization

$$s = \frac{(1-p)^2\,.\,p^*}{(1-p^*)^2\,.\,p} \qquad (24)$$

where p^* is the lowest value of p which satisfies equation (23) for a given value of β. The factor β describes the relationship between the distributions of finite molecular species pre- and post-gel. Before the gel point, $p = p^*$ and β increases with increasing p, reaching a maximum value at the gel point ($d\beta/dp = 0$ at $p = 1/(f-1)$, equation (23)). For $p > 1/(f-1)$ (post-gel) β and p^* decrease with increase in p, producing a reversion in the distribution of finite molecular species. p and p^* may be considered as conjugate extents of reaction, pre- and post-gel, respectively. Equation (24) shows that $s = 1$ before the gel point ($p^* = p$ and $g = 0$), decreasing post-gel to $s = 0$ at $p = 1$ ($p^* = 0$ and $g = 1$). The decrease in s after the gel point reflects the existence of a gel molecule of infinite molecular size (with an infinite number of reactive sites) which grows at the expense of the finite sol species. As $f_{\mathrm{w}} = 7550$, $p_{\mathrm{g}} = 1.325 \times 10^{-4}$ (equation (19)). To evaluate s (and hence g), as a function of p, in the range $0 \leq p \leq 1$, equation (23) was first solved numerically for p^*, in the range $1/(f-1) \leq p \leq 1$. s was then determined via equation (24). All calculations were performed on an IBM 486SX personal computer.

Correlation of Flory–Stockmayer analysis

In order to compare the results of the FS analysis with the experimental gel-fraction data, p was converted to equivalent radiation dose, D_{FS}, via equation (18). The resulting FS curves, both in the presence of acetylene and *in vacuo*, are shown in *Figures 7* and *8* (curves 2), together with the respective experimental gel fraction data (points 1). The FS curves are shifted in a positive direction along the dose axis, compared to the respective experimental gel-fraction data. Therefore, the Ichikawa *et al.* $G(R)$ value[8] again predicts insufficient radicals to reproduce the experimental gel-fraction data via FS theory, because

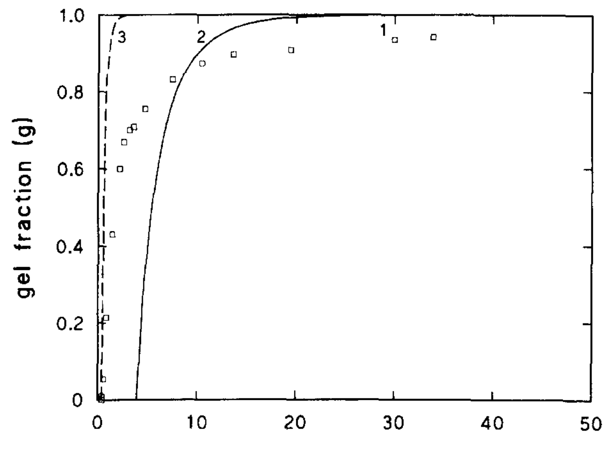

Figure 7 Gel-fraction *versus* dose plots for the acetylene enhanced irradiation of LLDPE, showing: (1) the experimental data (□); (2) the FS curve for f_w 7550, produced via equation (18) (——); and (3) the 'shifted FS curve' produced using constant $N_{CS.D_g}$ (equation (26)) applied to the entire dose range via equation (27) (– – –)

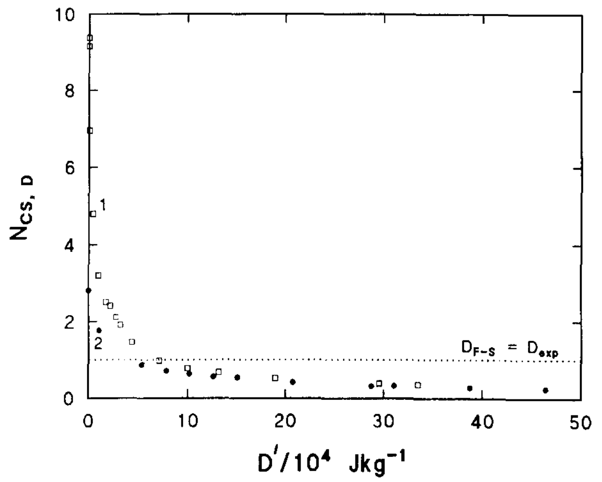

Figure 9 $N_{CS.D}$ ($=D_{FS}/D$) *versus* D' ($=D - D_g$) for given gel fractions from: (1) acetylene enhanced cross-linking (□); and (2) cross-linking *in vacuo* (●). The dotted line shows $D_{FS} = D$

of the presence of the chain reactions described earlier. This being the case, the experimental dose can be described in terms of the variables p and $N_{CS.D}$ by modifying equation (18) as follows

$$D = \frac{p}{N_{CS.D} \cdot G(R) \, . \, M_{CH_2}} = \frac{D_{FS}}{N_{CS.D}} \qquad (25)$$

Initially the FS gel-fraction *versus* dose curves were shifted, so that the predicted FS gel points (D_{FS,D_g}) coincided with the experimental gel points ($D_g \approx 0.42 \times 10^4$ and 1.40×10^4 Gy for in acetylene and *in vacuo* respectively). N_{CS,D_g} the number of 'gel-effective' chain steps at the gel point, was obtained by substituting D_g for D and p_g for p in equation (25), which gives

$$N_{CS.D_g} = \frac{p_g}{D_g \, . \, G(R) \, . \, M_{CH_2}} \qquad (26)$$

It can be seen from *Figure 9*, that the $N_{CS.D_g}$ value determined for the acetylene-gassed system (ca. 9.4) was much higher than that determined *in vacuo* (ca. 2.8), because of the nature of the two different sets of chain reactions discussed earlier. Also, the FS N_{CS,D_g} values compare favourably with those determined via the atomistic analysis (ca. 9.0 and 2.9 respectively). Use of the $N_{CS.D_g}$ values in equation (25) gives

$$D_{FS.g} = \frac{p}{N_{CS.D_g} \, . \, G(R) \, . \, M_{CH_2}} \qquad (27)$$

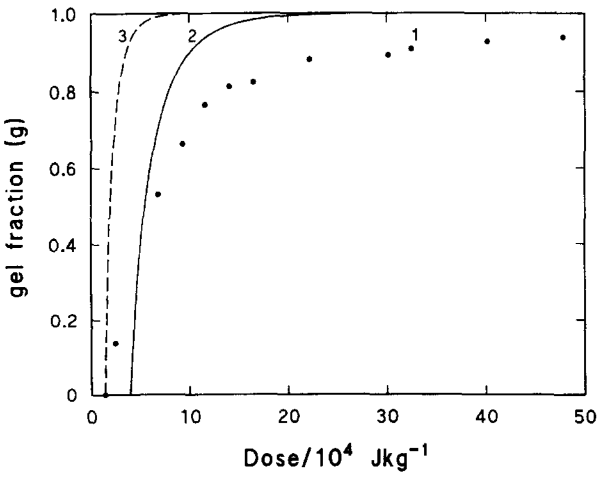

Figure 8 Gel fraction *versus* dose plots for the *in-vacuo* irradiation of LLDPE, showing: (1) the experimental data (●); (2) the FS curve for f_w 7550, produced via equation (18) (——); and (3) the 'shifted FS curve' produced using constant $N_{CS.D_g}$ (equation (26)) applied to the entire dose range via equation (27) (– – –)

The resulting shifted FS gel-fraction plots ($D_{FS,g}$) are also shown in *Figures 7* and *8* (curves 3). The initial slopes of both are greater than those of the experimental curves. The shifted curve for acetylene is closer to experimental observation than the *in-vacuo* one. However, subsequent to the initial region, the shifted FS curves do not fit the experimental data, because the values of N_{CS,D_g} were applied as constant factors over the whole dose region assuming that the efficiency of the chain-reactions was dose independent.

To illustrate the decay in $N_{CS,D}$ from the gel point onwards, the values required to reproduce all the experimental gel-fraction vs dose data were determined using equation (25) to give

$$N_{CS.D} = \frac{D_{FS}}{D} \qquad (28)$$

The results are shown in *Figure 9*, where $N_{CS,D}$ is expressed as a function of D', the dose in excess of that required for gelation ($D' = D - D_g$), for both the *in-vacuo-* and acetylene-incorporated experiments. In both cases, the maximum value of $N_{CS,D}$ occurs at the gel-point ($D' = 0$). As evaluated using equation (26) above, the $N_{CS.D}$ maxima were found to be ca. 9.4 in acetylene and 2.8 *in vacuo*.

In *Figure 9*, the $N_{CS,D}$ curves decrease sharply from the maximum values. For both sets of data, the effective concentrations of radicals required to emulate the chain-reactions, are greater than those given by $G(R)$ alone, at and some way beyond D_g. The values of $N_{CS,D}$ are equal to unity ($D_{FS}/D = 1$), at D' values of ca. 7.4×10^4 and 4.1×10^4 Gy, for the acetylene and *in-vacuo* systems respectively, corresponding to the point at which the FS curves (2) cross the curve of the experimental data (1)

(*Figures 7* and *8*). Values of $N_{\mathrm{CS,D}} = 1$ were not observed in the atomistic treatment until much higher doses were reached.

Further increases in D' result in decreases in $N_{\mathrm{CS,D}}$ to below unity ($D_{\mathrm{FS}}/D < 1$) in both systems. This may be due to non-crosslinking radical reactions occurring e.g. formation of in-chain unsaturation. Such reactions would be less affected than inter-chain reactions by the loss of chain-network mobility in the growing network. The two $N_{\mathrm{CS,D}}$ *versus* D' plots in *Figure 9* eventually converge at $D' \approx 15.0 \times 10^4$ Gy, indicating that the presence of acetylene has no additional effect on network formation beyond this value of D'.

At radiation doses beyond the gel point, the proportional decrease in the number of chain-steps relative to that at the gel point ($N_{\mathrm{CS,D}}/N_{\mathrm{CS,D_g}}$), can be analysed kinetically. If $N_{\mathrm{CS,D}}/N_{\mathrm{CS,D_g}}$ is assumed to follow nth-order kinetics after the gel-point, then

$$-\frac{d\{N_{\mathrm{CS,D}}/N_{\mathrm{CS,D_g}}\}}{dD'} = k_n \cdot \{N_{\mathrm{CS,D}}/N_{\mathrm{CS,D_g}}\}^n \quad (29)$$

where k_n is the nth-order rate constant with respect to D'. Integrating equation (29) with respect to D', over the range $N_{\mathrm{CS,D_g}}$ to $N_{\mathrm{CS,D}}$, yields an expression for D'

$$k_n . D' = \frac{1}{n-1} \cdot \{(N_{\mathrm{CS,D}}/N_{\mathrm{CS,D_g}})^{1-n} - 1\} \quad (30)$$

In *Figure 10*, $N_{\mathrm{CS,D}}/N_{\mathrm{CS,D_g}}$ is plotted as a function of D', for irradiations carried out both *in vacuo* and in acetylene. The dashed curves resulting from numerical fittings of the function in equation (30) provide good approximations of the experimental plots. The values of n and k_n were found to be 2.83 and $3.39 \times 10^{-4}\,\mathrm{Gy}^{-1}$ respectively in acetylene, and 2.65 and $0.65 \times 10^{-4}\,\mathrm{Gy}^{-1}$ respectively *in vacuo*. The decays in the number of 'gel-effective' chain-steps are thus approximately third-order with respect to dose in excess of that required for gelation. Although the physical meaning of the values of n remains unclear, the rate constant (k_n), is higher for the irradiation carried out in acetylene, as expected, due to the greater initial shift required to fit the FS curve at the gel point in acetylene (i.e. higher $N_{\mathrm{CS,D_g}}$), relative to the case *in vacuo*. The curves in *Figure 10* do not converge with increasing dose (cf. *Figure 9*), because the ordinate now measures the proportional decrease in the number of 'gel-effective' chain-steps, relative to the value at the gel point. The differences between the two curves at larger radiation doses therefore reflect the greater number of 'gel-effective' chain-steps in the acetylene system.

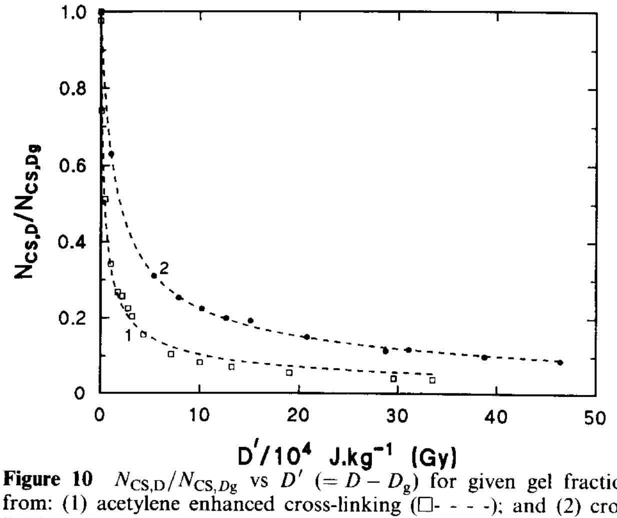

Figure 10 $N_{\mathrm{CS,D}}/N_{\mathrm{CS},D_g}$ vs D' ($= D - D_g$) for given gel fractions from: (1) acetylene enhanced cross-linking (□- - - -); and (2) cross-linking *in vacuo* (●- - - -)

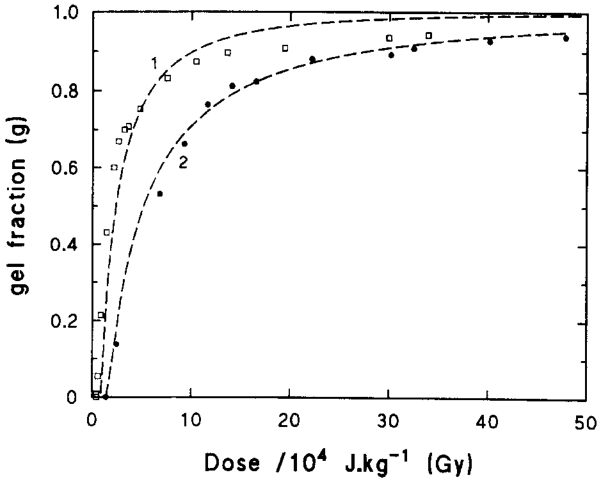

Figure 11 Experimental gel-fraction data fitted to equation (31) for: (1) acetylene enhanced crosslinking (□ - - - -); and (2) cross-linking *in vacuo* (● - - - -)

Finally, $N_{\mathrm{CS,D}}/N_{\mathrm{CS,D_g}}$ in equation (30) was replaced by $D_{\mathrm{FS,g}}/D$ using equations (18), (25) and (27)

$$k_n . D' = \frac{1}{n-1} \cdot \{(D_{\mathrm{FS,g}}/D)^{1-n} - 1\} \quad (31)$$

Equation (31) was then solved numerically, using the method of binary subdivision, to yield the value of D' (or D) for a given $D_{\mathrm{FS,g}}$. These values of D' were used to scale the abscissae of the D_g coincident FS curves for the experiments in acetylene and *in vacuo* (*Figures 7* and *8* respectively, curves 3), to account for the decay in number of effective chain-steps after the gel point. The resulting curve-fits are shown in *Figure 11*, and are seen to provide reasonable approximations to the experimental data, as they should. In acetylene, the discrepancies between the fitted curve and experimental data points at higher doses, caused by larger predicted values of $N_{\mathrm{CS,D}}/N_{\mathrm{CS,D_g}}$ compared with experiment in *Figure 10*, are thought to be due to the poor numerical fit of an nth order decay equation to the $N_{\mathrm{CS,D}}/N_{\mathrm{CS,D_g}}$ *versus* D' data rather than a failure of FS theory.

CONCLUSIONS

Crosslinking of LLDPE by irradiation and annealing at 100°C, both *in vacuo* and in the presence of acetylene, results in lower radiation doses to gelation and higher gel-fractions for a given dose, than those predicted by either FS theory or the theoretical maximum obtainable assuming every radical reacts to form a crosslink ($D . G(R)/2$). Comparisons of both the atomistic computer analysis and the FS numerical analysis with experiment confirm that chain-reactions provide the only satisfactory explanation for the higher experimental observations (*Schemes 3* and *4*). The presence of chain-reactions is the reason why empirical formulae developed to date do not describe fully the gel fractions obtained from the radiation-induced crosslinking of polymers.

The FS analysis indicates that the chain-reactions are most efficient at the gel point, giving rise to a maximum number of gel-effective chain-steps ($N_{\mathrm{CS,D}}$(max)) of ca. 9.4 in acetylene and ca. 2.8 *in vacuo*. Hence, the number of effective chain-reactions generated per radical at the gel point in the presence of acetylene is more than three times larger than *in vacuo*. The FS analysis also suggests that at doses beyond the gel point, $N_{\mathrm{CS,D}}$ decreases rapidly with continuing irradiation, until at doses exceeding ca. 15×10^4 Gy, the acetylene appears to have no additional effect on gel formation when compared to the *in vacuo* case. Further to this, at doses in excess of ca. 35×10^4 Gy, $N_{\mathrm{CS,D}}$ remains essentially constant. Hence, the effects of the chain-reactions appear to be balanced by factors which prevent crosslinking reactions such as the formation of in-chain unsaturation. The decrease in $N_{\mathrm{CS,D}}$ were found to be approximately 2.6th and 2.8th order, with respect to D', in acetylene and *in vacuo* respectively.

The atomistic analysis, on the other hand, indicates that the chain-reactions are most efficient at doses a little way beyond the gel point, but yields similar $N_{\mathrm{CS,D}}$(max) values of ca. 9.0 and 2.9 for acetylene and *in vacuo* respectively. This analysis also suggests that acetylene continues to increase gel formation until a dose of 45×10^4 Gy is reached. For the *in vacuo* case there appears to be a smaller increase, hence, acetylene is more effective than molecular hydrogen in inducing crosslinking up to this dose. Unlike the FS analysis, in the atomistic model the effects of the chain-reactions do not appear to be cancelled out by factors which prevent crosslinking, under either of the conditions, although such decreases may occur at doses greater than 55×10^4 Gy. Analysis of the interpolated $N_{\mathrm{CS,D}}$ dose curves, developed via atomistic modelling, demonstrates a clear relationship between the number of 'gel-effective' chain-steps and the dose for both acetylene incorporated and *in vacuo* irradiations (equation (5)). $N_{\mathrm{CS,D}}$ appears to increase prior to $N_{\mathrm{CS,D}}$(max), as approximately a 0.7th order reaction with respect to dose for both conditions. Beyond $N_{\mathrm{CS,D}}$(max), $N_{\mathrm{CS,D}}$ appears to decrease approximately as second order (2.1th-order) with respect to dose in acetylene. This results from the increased probability of radical–radical terminations at higher doses. The decrease of $N_{\mathrm{CS,D}}$ *in vacuo*, was found to be approximately 2.6th order with respect to dose. This increase from second-order may result from the interference of termination reactions with chain-scissions. In the atomistic model, the relationships between the gel fraction and the number of 'gel-effective' crosslinks per pre-irradiated number-average molecule has been obtained for both *in vacuo* and acetylene irradiations (equation (12)). As the gel fraction increases, the number of 'gel-effective' crosslinks required to achieve it increases exponentially from the minimum possible statistical arrangement. It can be considered that for any number of 'gel-effective' crosslinks there are many ways of arranging them between the initial number-average molecules. In the atomistic model for any given gel fraction, a minimum statistical arrangement occurs when all the crosslinked molecules are connected once only to one other molecule. However, as the gel fraction increases the probability that a minimum statistical arrangement will be achieved becomes very much smaller due to multiple connections. Hence, to achieve higher gel fractions a greater number of crosslinks than the statistical minimum are required. The number of crosslinks required, or the deviation from the statistical minimum gradient (*Figure 4*), increases exponentially with increasing gel fraction. This exponential increase is primarily related to the number of pre-irradiated chains per unit volume, or the initial degree of polymerization. It is probably also related to spatial and physical arrangements of the pre-irradiated polymer molecules, such as end-to-end length, branching, folding and crystallinity.

Both methods of analysis allow us to relate the gel fraction to dose and the number of initial radicals generated in a pre-irradiated number-average or weight-average degree of polymerization, via $N_{\mathrm{CS,D}}$ (equation (14) and (14.1), atomistic method, and equations (28) and (30), FS method). These equations are an improvement on current gel-fraction equations, used in studying radiation effects of polymers, because they take account of chain-reactions. Essentially, the two theoretical analyses are in close agreement in their interpretation of the region at the gel point and a little way beyond. As the dose is increased further beyond the gel point, the two interpretations become more divergent. This divergence arises because of the inherent differences in the basic assumptions of the two approaches. The atomistic modelling technique assumes that all crosslinks are capable of contributing to the gel. FS theory, on the other hand, assumes that gelation does not occur until an infinite molecular growth is achieved, because there is a very high number of potential sites for crosslinking (high chemical functionality), p_g is very small, and the differences between the atomistic and FS models are small near the gel point.

For the case where acetylene is present, our previous research on polyene crosslinks is not invalidated by the presence of chain-reactions[1,11,12]. The polyene crosslinks do exist and they result from radical–radical chain termination reactions. The total number of crosslinks however, is much higher than we had supposed from the polyene terminations alone. At 18×10^4 Gy, the total number of crosslinks is likely to be at least ca. four times greater than previously measured by u.v.-spectroscopy as inter-chain polyenes. The hydrogen atom abstraction reaction discovered in our *FT*i.r. work[12] forms the starting point of the chain reaction. In the *FT*i.r. experiments the quantity of *trans*-olefin measured, at any given dose, was always in excess of that attributable to the terminating polyenes[1]. Previously we had thought that the excess *trans*-olefin existed largely inter-chain, however, we now believe it results from the chain reaction in acetylene. Radical addition to vinylic non-chain-bridging polyenes, destroys the polyenes, but not their capability to crosslink, leaving behind semi-saturated systems as isolated *trans*-olefins. The decrease in the rate of vinyl formation, also measured by *FT*i.r., is likewise in keeping with the reduction of hydrogen atom abstraction and the chain reactions observed here.

For *in-vacuo* irradiation, the chain reaction involves mainly molecular hydrogen and some excised low alkyls. Since the volume immediately outside the polymer is evacuated, the shape, bulk density and excess vessel volume may affect the extent of this *in-vacuo* chain reaction. Where molecular hydrogen is easily lost to a void, the chain reaction may become reduced.

Conversely, the extent of the *in-vacuo* chain reaction might be increased by adding molecular hydrogen or low alkyls, although this is unlikely to reach the effectiveness of acetylene, because the former relies upon vinyl forming chain scission events. The *in-vacuo* excess *trans*-olefin observed during our *FT*i.r. work[12] is probably not inter-chain, because the chain reaction uses up the unsaturation generated during chain scission and there is little or no excess available. It is more likely that it results from movement of radicals adjacent to each other during simple chain-steps. Since terminal vinyl groups were never observed by *FT*i.r., the capacity of the *in-vacuo* chain-reactions for removing them was demonstrated.

ACKNOWLEDGEMENTS

Richard Jones would like to thank the Hoechst-Celanese Corporation for their continuing support of his work, David Taylor acknowledges support from the EPSRC (Grant No. GR/J/24935).

REFERENCES

1 Jones, R. A., Salmon, G. A. and Ward, I. M. *J. Polym. Sci., Polym. Phys. Edn* 1993, **31**, 807

2 Charlesby, A. *Proc. Royal. Soc. A* 1954, **222**, 542

3 Charlesby, A. and Pinner, S. H. *Proc. Royal Soc. A* 1959, **249**, 367

4 Saito, O., Kang, H. and Dole, M. *J. Chem. Phys.* 1996, **46(9)**, 3607

5 Kang, H. Y., Saito, O. and Dole, M. *J. Am. Chem. Soc.* 1967, **89(9)**, 1980

6 Jones, R. A. *J. Polym. Sci., Polym. Phys. Edn* 1994, **32**, 2049

7 Wanxi, Z., Tianbai, H., Jiazhen, S. and Baogong, Q. *Radiat. Phys. Chem.* 1989, **33(6)**, 581

8 Ichikawa, T., Kawahara, S. and Yoshida, H. *Radiat. Phys. Chem.* 1985, **26(9)**, 731

9 Jones, R. A., Taylor, D. J. R., Stepto, R. F. T. and Ward, I. M. *J. Polym. Sci., Polym. Phys. Edn*, 1996, **34**, 901

10 Bowmer, T. N. and O'Donnell, J. H. *Polymer* 1977, **18**, 1032

11 Jones, R. A., Salmon, G. A. and Ward, I. M. Radiation Effects on Polymers: Chem. and Tech. Aspects, ACS 208th Symposium, 21st–25th Aug., 1994, to be pub. *Polym. Prepr.* (1995) (Abs. of Papers of the Am. Chem. Soc., 208, 2, p 312 – Poly. (1994)).

12 Jones, R. A., Salmon, G. A. and Ward, I. M. *J. Polym. Sci., Polym. Phys. Edn* 1994, **32**(3), 469

13 Dubinskii, A. A., Grinberg, O. Ya., Tabachnik, A. A. and Lebedev, Ya. S. *High Energy Chem.* 1977, **11(2)**, 125

14 Iwasaki, M., Ichikawa, T. and Ohmori, T. *J. Chem. Phys.* 1969, **50(5)**, 1991

15 Stockmayer, W. H. *J. Polym. Sci.* 1953, **11**, 424

16 Stepto, R. F. T. in 'Comprehensive Polymer Science', 1st Suppl. (Eds S. L. Aggarwal and S. Russo), Pergamon Press, Oxford, 1992, Chapter 10

17 Polymer Module, Version 6, Biosym Technologies Inc., San Diego, CA, USA, 1994.

18 Patel, G. N. and Keller, A. *J. Polym. Sci., Polym. Phys. Edn* 1975, **13**, 323

19 Dole, M. in 'Advances in Radiation Chemistry', (Eds M. Burton and J. L. Magee), 4th Edn, Wiley, London, 1974, p. 340

20 Jones, R. A., Orchard, G. A. J. and Ward, I. M. *J. Appl. Polym. Sci.* 1992, **45**, 819